Introduction and overview of nuclear shapes and radial structures

Michael Bender

Institut de Physique des 2 Infinis de Lyon
CNRS/IN2P3 & Université de Lyon & Université Lyon 1
F–69622 Villeurbanne, France

Physics Opportunities from the RHIC Isobar Run

RIKEN BNL Research Center
held virtually January 25-28, 2022

The concept of intrinsic shapes

The concept of the "intrinsic shape" of an atomic nucleus refers to

- the geometric arrangement of nucleons
- a non-observable feature of the nucleus' wave function
- the interpretation of nuclear observables in terms of a classical picture

Setting the frame I: Symmetries

Noether's first theorem: "Every differentiable symmetry of the action of a physical system with conservative forces has a corresponding conservation law."

E. Noether, Nachr. Ges. Wiss. Göttingen, Math. Phys. Kl. 1918, 235.

Symmetries of the nuclear Hamiltonian and

- Translational invariance
- Galilean/Lorentz invariance
- Time-translational invariance
- Rotational invariance
- Time-reversal invariance
- Space-inversion invariance
- Global gauge invariance

Note: "invariance" does **not** mean that the nuclear many-body wave function does not change under such transformation, but that it transforms according to the rules of group representation theory for the group associated with the respective symmetry transformation.

Setting the frame I: Symmetries

Nuclei are isolated self-bound systems (with some Symmetries of the nuclear Hamiltonian:

- Translational invariance $\Rightarrow$ momentum conservation
- Galilean/Lorentz invariance $\Rightarrow$ only center-of-mass momentum changes when changing inertial frame
- Time-translational invariance $\Rightarrow$ angular energy conservation
- Rotational invariance $\Rightarrow$ angular-momentum conservation
- Time-reversal invariance (no quantum number associated with anti-linear operators)
- Space-inversion symmetry $\Rightarrow$ parity conservation
- Global gauge invariance $\Rightarrow$ particle-number conservation

There are quantum numbers of the nuclear many-body state associated with the conserved quantities.

These symmetries have a number of important consequences

- Conserved quantum numbers lead to selection rules for expectation values and transition matrix elements.
- Symmetries introduce *correlations* in the nuclear many-body wave function, such that the nucleons cannot evolve each independently from one another.
- A useful, but not conserved symmetry is the one under transformation in isospin space, which leads to approximate isospin quantum numbers (broken mainly by electromagnetic interactions, and on a much lesser level also by small differences in the strong interaction between nucleons).

- The features of the nucleon-nucleon interactions have as a consequence that nucleons of the same species tend to couple pairwise to pairs with $L = 0$, $S = 0$.
  - $\Rightarrow$ ground states of even-even nuclei have angular momentum $J = 0$ and parity $\pi = +1$.
  - $\Rightarrow$ angular momentum and parity of the ground state of an odd-mass nucleus determined by "unpaired" nucleon, $J^\pi = 1/2^\pm, 3/2^\pm, 5/2^\pm, \ldots$
  - $\Rightarrow$ angular momentum and parity of the ground state of an odd-odd nucleus determined by the coupling of the "unpaired" proton and neutron, $J^\pi = 0^\pm, 1^\pm, 2^\pm, 3^\pm, \ldots$
- From the rules of angular-momentum and parity coupling follows that
  - the multipole moments $\hat{Q}_{\ell m}$ of the *ground states* of even-even nuclei are all zero for any $\ell > 0$

$$\langle 0^+ | \hat{Q}_{\ell m} | 0^+ \rangle = 0$$

  - the ℓ moment of excited states of even-even nuclei, and states of odd- and odd-odd nuclei can be measured if ℓ is even and J sufficiently large

$$\langle J^\pi | \hat{Q}_{\ell m} | J^\pi \rangle \neq 0 \quad \text{if } J \geq \ell/2 \text{ and } \ell \text{ even}$$

  - The diagonal matrix elements of all odd-ℓ multipole moments is zero

$$\langle J^\pi | \hat{Q}_{\ell m} | J^\pi \rangle = 0 \quad \text{if } \ell \text{ odd}$$

Transition matrix elements of multipole moment operators between states are in general non-zero

- even parity multipole moments $\ell = 2n \geq 2$ (quadrupole, hexadecapole, ...)

$$\langle J_f^{\pm} | \hat{Q}_{\ell m} | J_i^{\pm} \rangle \neq 0$$

- because the photon has spin 1, there are no electromagnetic $E0$ transitions that lead to γ emission

$$\langle J^{\pm} | \hat{Q}_{00} | J^{\pm} \rangle = 0$$

(but there are $E0$ transitions via conversion-electron spectroscopy, for which the transition operator is r^2)

- odd parity multipole moments $\ell = 2n + 1$ (dipole, octupole, ...)

$$\langle J_f^{\mp} | \hat{Q}_{\ell m} | J_i^{\pm} \rangle \neq 0 \quad \text{if } |J_i - J_f| \geq \ell/2 \text{ and } \ell \text{ odd}$$

The reduced $E2$ transition probability is given by

$$B(E2; J'_{\nu'} \to J_\nu) = \frac{e^2}{2J'+1} \sum_{M=-J}^{+J} \sum_{M'=-J'}^{+J'} \sum_{\mu=-2}^{+2} |\langle JM\nu | \hat{Q}_{2\mu} | J'M'\nu' \rangle|^2$$

$$= \frac{e^2}{2J'+1} \left| \langle J\nu || \hat{Q}_2 || J'\nu' \rangle \right|^2$$

The spectroscopic quadrupole moment is given by

$$Q_s(J) = \sqrt{\frac{16\pi}{5}} \langle JJ\nu | \hat{Q}_{2\mu} | JJ\nu \rangle$$

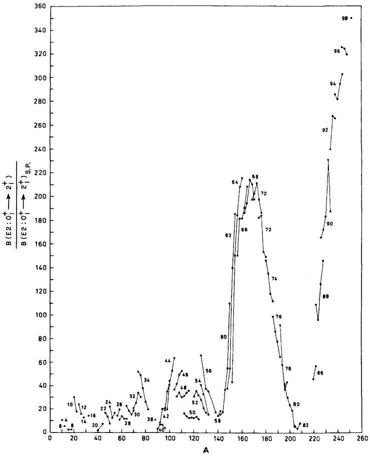

Fig. 2.16. B(E2:$0^+_1 \rightarrow 2^+_1$) values for all even–even nuclei. (Bohr, 1975.)

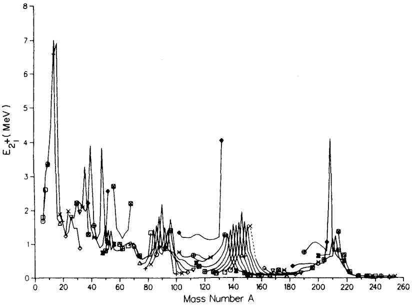

Fig. 2.12. $E_{2^+_1}$ values for all even–even nuclei (Raman, 1987).

$$E_J = \frac{J(J+1)}{2\Theta}$$

where Θ is the nuclear rotational moment of inertia, that grows with deformation.

These are "old" plots to avoid overlapping structures visible when plotting all of today's available data

taken from R. Casten, "Nuclear Structure from a Simple Perspective", Oxford University Press (1990)

Schematic attribution of an intrinsic multipole moment to a multipole moment measured in the laboratory

B. Rotational model.—The phenomenological Hamiltonian for a system in which a number of nucleons are coupled to a rotator is written as

$$H = \sum_\nu \frac{\hbar^2}{2\mathfrak{I}_\nu}(I_\nu - J_\nu)^2 + H_{int} \qquad \text{V.9.}$$

where $\mathfrak{I}_\nu$, I_ν, and J_ν are the νth component of the moment of inertia, of the total angular momentum, and of the intrinsic angular momentum respectively. The last quantity is a sum of individual nucleons. The last term in Equation V.9 is the intrinsic Hamiltonian which represents the intrinsic motion. In this section the rotational motion for axially symmetric shapes is considered:

$$\mathfrak{I}_1 = \mathfrak{I}_2 = \mathfrak{I} \qquad \text{V.10.}$$

The corresponding wavefunction is given by

$$\Psi_{IMK} = \sqrt{\frac{2I+1}{16\pi^2(1+\delta_{K,0})}} \cdot \left[\mathfrak{D}_{MK}{}^I(\theta_i)\chi_K + (-)^{I+K}\mathfrak{D}_{M-K}{}^I(\theta_i)\,\mathfrak{R}_2(\pi)\chi_K\right] \qquad \text{V.11.}$$

where $\mathfrak{D}_{MK}{}^I(\theta_i)$ is the rotational matrix, K is the third component of the total angular momentum while χ_K is the intrinsic wavefunction, and the eigenvalue of J_3 is assumed to be K. The operator $\mathfrak{R}_2(\pi)$ represents the rotation by π around the second coordinate axis.

taken from S. Yoshida & L. Zamick, Ann. Rev. Nucl. Sci 22 (1972) 121

In general the electromagnetic moment is now written in the rotating coordinate system

$$\mathfrak{M}(\lambda, \mu) = \sum_\nu \mathfrak{D}_{\mu\nu}{}^\lambda(\theta_i)\mathfrak{M}'(\lambda, \xi) \qquad \text{V.12.}$$

where $\mathfrak{M}'(\lambda, \nu)$ is the moment in the rotational coordinate system. In general the reduced transition rate is given as

$$B(\lambda; I_iK_i \to I_fK_f) = \frac{1}{2I_i+1}\left|\langle I_fK_f \| \mathfrak{M}'(\lambda) \| I_iK_i\rangle\right|^2 \qquad \text{V.13.}$$

where

$$\begin{aligned}
&\langle I_fK_f \| \mathfrak{M}'(\lambda) \| I_iK_i\rangle \\
&= (2I_i+1)^{\frac{1}{2}}[(I_iK_i\lambda K_f - K_i \mid I_iK_i)\langle K_f \mid \mathfrak{M}'(\lambda, K_f - K_i) \mid K_i\rangle \qquad \text{V.14.}\\
&+ (-)^{I_i-K_i}(I_i - K_i\lambda K_i + K_f \mid I_fK_f)\langle K_f \mid \mathfrak{M}'(\lambda, K_i + K_f) \mid K_i\rangle].
\end{aligned}$$

(Spherical) vibrator:

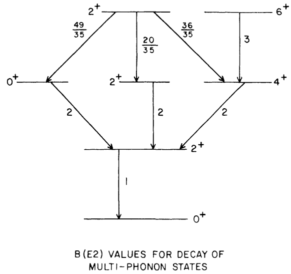

Fig. 6.4. B(E2) values in the harmonic vibrator model.

transition moments are relative to $B(E2, 2_1^+ \rightarrow 0_1^+)$

Deformed rotor as a function of triaxiality γ

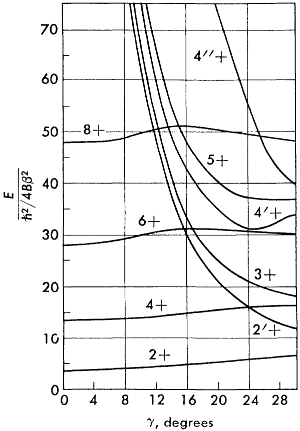

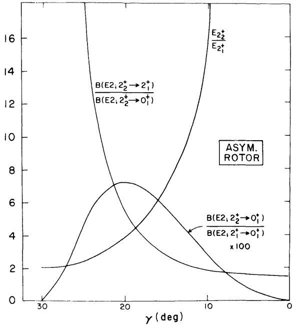

Fig. 6.19. Dependence of several observables on γ (compare Fig. 6.42).

Note: in microscopic models, the spectra might evolve quicker with γ

Note: real nuclei are more complicated, as are spectra predicted by microscopic models

taken from R. Casten, "Nuclear Structure from a Simple Perspective", Oxford University Press (1990)

Deformed odd nuclei

- Another phenomenon that is sensitive to deformation are the coexisting rotational bands of odd-mass nuclei.
- Coupling of single-particle states to a deformed rotational core
- Successful modeling requires internal consistency of deformed single-particle spectrum, moment of inertia of rotational motion and electromagnetic moments of in-band transitions.
- Similar (but more complicated) for odd-odd nuclei and single-particle excitations in even-even nuclei.

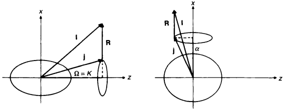

Fig. 11.3. Schematic illustration of the two extreme coupling schemes; deformation alignment (left figure) and rotation alignment (right figure) (from R.M. Lieder and H. Ryde, *Adv. in Nucl. Phys.*, eds. M. Baranger and E. Vogt (Plenum Publ. Corp., New York) vol. 10 (1978) p. 1).

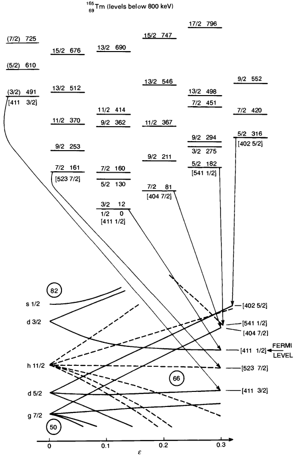

Fig. 11.4. For legend see opposite.

taken from S. G. Nilsson & I. Ragnarsson, "Shapes and Shells in Nuclear Structure", Cambridge University Press (1995).

Charge density $\neq$ proton density

- Coupling to electromagnetic fields
  - $\Rightarrow$ measures charge distribution $\neq$ proton distribution
  - because of their substructure, protons and neutrons have an intrinsic charge distribution of finite size
  - because of electromagnetism being manifestly Lorentz-covariant, there are relativistic corrections to the charge density, such as a contribution from the coupling to the divergence of the spin current, $\boldsymbol{\nabla} \cdot \mathbf{J}$ of protons and neutrons, a Darwin correction etc

intrinsic charge distribution of a proton and a neutron

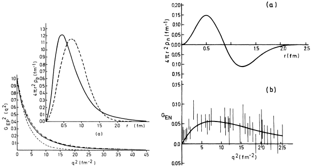

charge distribution of ^{208}Pb

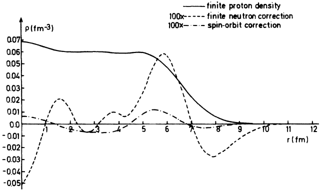

Chandra et al, PRC 13 (1976) 245

Another indicator of deformation: systematics of (charge) radii

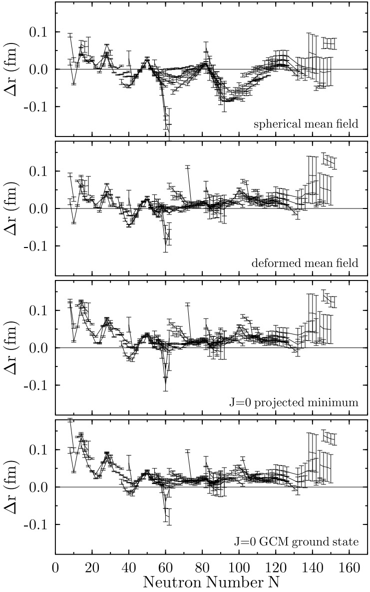

⇐ difference between calculated and experimental charge radius at four levels of modelling (from spherical mean field to symmetry-restored beyond-mean-field with shape fluctuations)

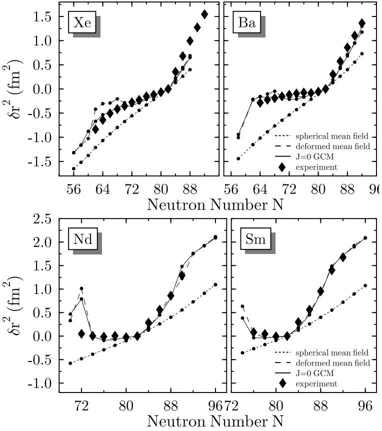

M. B., G. F. Bertsch and P.-H. Heenen, Phys. Rev. C 69 (2004) 034340

Beware of coexisting conventions - Experiment

Cartesian vs spherical multipole moments

- Atomic physicists prefer to work with cartesian multipole tensors or an expansion in Legendre polynomials, for example

$$Q_0 = \int d^3r \, \rho(\mathbf{r}) \big(3z^2 - \mathbf{r}^2\big) = \sqrt{\frac{5}{16\pi}} \, Q_{20} \qquad \text{(axial quadrupole moment)}$$

- Nuclear spectroscopists prefer to work with spherical tensors, for example

$$Q_{20} = \int d^3r \, \rho(\mathbf{r}) \, r^2 \, Y_{20}(\mathbf{r}) = \sqrt{\frac{16\pi}{5}} \, Q_0 \qquad \text{(axial quadrupole moment)}$$

  Note that there are also other definitions of spherical harmonics that differ in normalisation and phase convention.

- Dimensionless (charge) multipole moments

$$\beta_{\ell m} = \frac{4\pi}{3R^\ell Z} \, Q_{\ell m}$$

  where R is usually (but not always!) taken to be $R = 1.2 \, A^{1/3}$ fm

Position of the nuclear surface in terms of a multipole expansion

$$R(\vartheta, \varphi) = R_d[\{\alpha_{LM}\}]\Big[1 + \sum_{LM} \alpha_{LM} \, Y_{LM}(\vartheta, \varphi)\Big] .$$

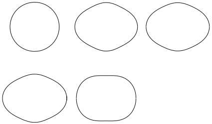

Assuming incompressible nuclear matter, $\rho = 3A/(4\pi R_0^3)$, and a sharp surface, the proportionality constant $R_d[\{\alpha_{LM}\}]$ is fixed by volume conservation

$$\begin{aligned} A &= \int_0^{2\pi} d\varphi \int_0^{\pi} d\vartheta \, \sin(\vartheta) \int_0^{R(\vartheta,\varphi)} dr \, r^2 \, \rho \\ &= \frac{A \, R_d^3[\{\alpha_{LM}\}]}{4\pi R_0^3} \int_0^{2\pi} d\varphi \int_0^{\pi} d\vartheta \, \sin(\vartheta) \, \Big[1 + \sum_{LM} \alpha_{LM} \, Y_{LM}(\vartheta, \varphi)\Big]^3 \end{aligned}$$

Multipole moments

$$\begin{aligned} \langle Q_{\ell m} \rangle &= \int_0^{2\pi} d\varphi \int_0^{\pi} d\vartheta \, \sin(\vartheta) \int_0^{R(\vartheta,\varphi)} dr \; r^2 \, \rho \, r^\ell \; Y_{\ell m}(\vartheta, \varphi) \\ &= \frac{3A}{4\pi R_0^3} \, \frac{R_d^{\ell+3}}{\ell + 3} \int_0^{2\pi} d\varphi \int_0^{\pi} d\vartheta \, \sin(\vartheta) \, Y_{\ell m}(\vartheta, \varphi) \, \Big[1 + \sum_{LM} \alpha_{LM} \, Y_{LM}(\vartheta, \varphi)\Big]^{\ell+3} \end{aligned}$$

For a purely quadrupole-deformed surface one has

$$R(\vartheta,\varphi) = R_d[\{\alpha_{LM}\}] \left[1 + \alpha_{20}\, Y_{20}(\vartheta,\varphi)\right]$$

$$R_d = R_0 \left(1 + \frac{3}{4\pi}\,\alpha_{20}^2 + \frac{1}{(4\pi)^{3/2}}\,\frac{6\sqrt{5}}{21}\alpha_{20}^3\right)^{-1/3} \simeq 1 - \frac{1}{4\pi}\,\alpha_{20}^2 - \frac{1}{(4\pi)^{3/2}}\,\frac{6\sqrt{5}}{21}\,\alpha_{20}^3$$

$$\beta_{20} = \frac{R_d^5}{R_0^5}\left(\alpha_{20} + \sqrt{\frac{5}{4\pi}}\,\frac{4}{7}\,\alpha_{20}^2 + \frac{5}{4\pi}\,\frac{6}{7}\,\alpha_{20}^3 + \frac{5}{4\pi}\,\sqrt{\frac{5}{4\pi}}\,\frac{20}{77}\,\alpha_{20}^4 + \cdots\right)$$

$$= \alpha_{20} + \sqrt{\frac{5}{4\pi}}\,\frac{4}{7}\,\alpha_{20}^2 - \frac{5}{4\pi}\,\frac{1}{7}\,\alpha_{20}^3 - \frac{5}{4\pi}\,\sqrt{\frac{5}{4\pi}}\,\frac{94}{231}\,\alpha_{20}^4 + \cdots$$

Expressions get much more complicated when the surface has also higher-order deformations.

Note: Experimentalists sometimes re-express their measurements for multipole moments in terms of surface deformation in a model-dependent way.

Do nuclei have *one* intrinsic shape?

- Shape fluctuations: nuclear wave function is spread over a large range of deformation
- Shape coexistence: two or several minima yielding states of different deformation in the same nucleus

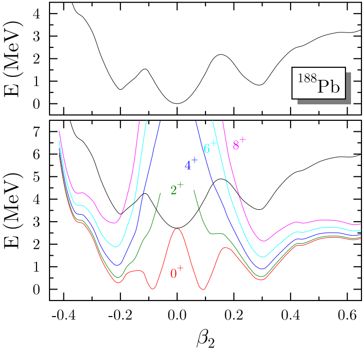

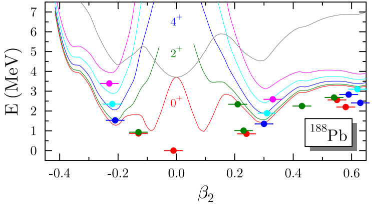

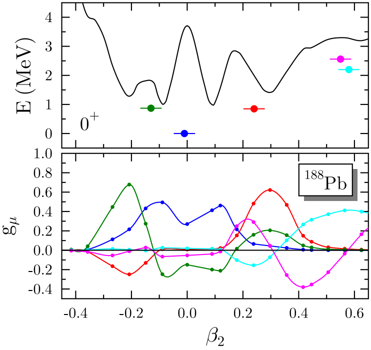

Bender, Bonche, Duguet, Heenen, PRC 69 (2004) 064303

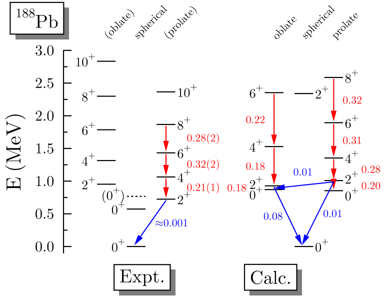

Bender, Bonche, Duguet, Heenen, PRC 69 (2004) 064303.
Experiment: Grahn *et al*, PRL **97** (2006) 062501

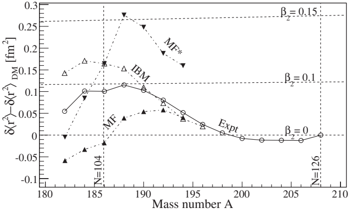

FIG. 3. Difference from the experimental mean square charge radii (Expt), the beyond mean-field calculations with normal [4] (MF) and decreased pairing [18] (MF*), and the IBM calculations (IBM) to the droplet model calculations for a spherical nucleus. Isodeformation lines from the droplet model at $\beta_2 =$ 0.1 and 0.15 are shown.

de Witte et al, PRL 98 (2007) 112502

Building models that use/employ/imply the concept of intrinsic shapes

- Self-consistent mean-field models (aka Hartree-Fock (HF), HF+BCS, Hartree-Fock-Bogoliubov (HFB), nuclear density functional theory, single-reference energy density functional method, ...)
- Auxiliary product states $|\Phi\rangle$ as fundamental building block $\Leftrightarrow$ assumption of independent single-particle (or independent quasiparticle) states

$$|\Phi_{\mathrm{HF}}\rangle = \prod_{k=1}^{A} \hat{a}_k^\dagger |-\rangle \qquad \text{or} \qquad |\Phi_{\mathrm{HFB}}\rangle = \prod_{k>0}$$

- Deformation energy landscapes can be constructed using constraints
- The experience of 50+ years of applications demonstrate that this approach describes many features of low-energy nuclear structure and some features of low-energy nuclear reactions.
- Symmetries can be restored with projection techniques $|\Phi\rangle$
- Shape fluctuations & shape coexistence can be modeled with configuration mixing (see some of the previous slides).

Scamps, Goriely, Olsen, Bender, Ryssens, EPJ A 57 (2021) 333

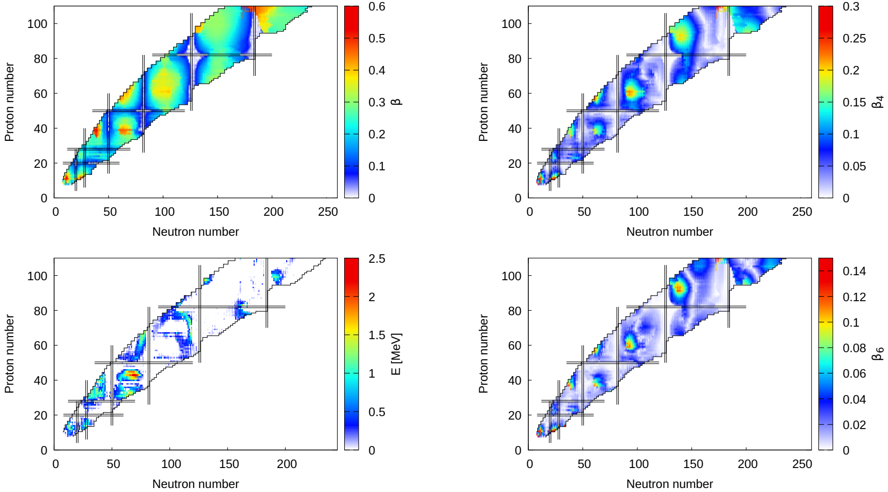

- Calculations assuming reflection symmetry
- ⇒ For systematics of reflection asymmetric shapes see talk by Luis Robledo

Scamps, Goriely, Olsen, Bender, Ryssens, EPJ A 57 (2021) 333

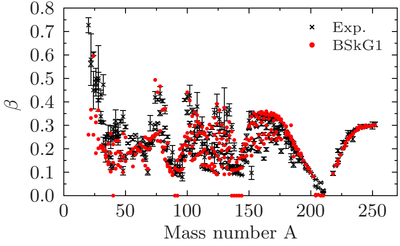

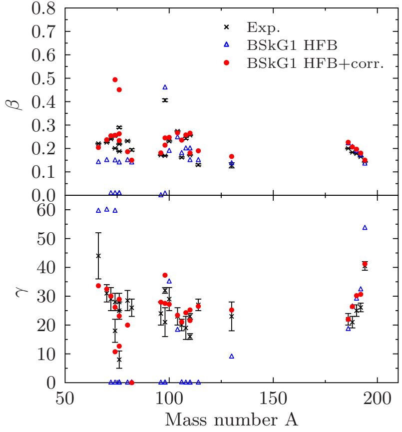

Coulomb excitation and shape invariants

borrowed from a talk by M. Zielinska

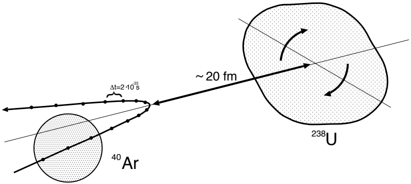

Idea: excite a nucleus in-flight by the electromagnetic potentials of another nucleus.

The Cline–Flaum sum rule [10,12,13]) is a model-independent and non-energy-weighted sum rule and provides an alternative and very useful means for examining the correlations among the E2 data. In analogy to the Bohr parameters (β, γ), the E2 operators in the intrinsic frame are parameterized with (Q, δ) under this sum rule.

$$E_{2,0} = Q\cos\delta\,, \qquad E_{2,\pm1} = 0\,, \qquad E_{2,\pm2} = \sqrt{\tfrac{1}{2}}Q\sin\delta\,. \tag{4}$$

The zero-coupled products of the E2 operators can be expressed in terms of Q and δ, e.g.,

$$[\mathrm{E2}\times\mathrm{E2}]^0 = \sqrt{\tfrac{1}{5}}Q^2\,, \qquad [[\mathrm{E2}\times\mathrm{E2}]^2\times\mathrm{E2}]^0 = \frac{1}{\sqrt{2/35}}Q^3\cos(3\delta)\,. \tag{5}$$

The expectation values of matrix elements for these rotationally invariant zero-coupled products for a given state s can be evaluated using an intermediate state expansion, e.g.,

$$\langle \mathrm{s}|[\mathrm{E2}\times\mathrm{E2}]^J|\mathrm{s}\rangle = \frac{(-1)^{I_s+I_s}}{(2I_s+1)^{1/2}}\sum_{\mathrm{t}}\langle \mathrm{s}|E2|\mathrm{t}\rangle\langle \mathrm{t}\|E2\|\mathrm{s}\rangle \begin{Bmatrix} 2 & 2 & J \\ I_s & I_s & I_t \end{Bmatrix}\,, \tag{6}$$

where

$$\begin{Bmatrix} 2 & 2 & J \\ I_s & I_s & I_t \end{Bmatrix}\,,$$

is the Wigner $6j$ symbol. Thus the expectation values of (Q, δ) for a state are determined from a set of E2 matrix elements according to eq. (6) and the like. There are different ways to evaluate (Q, δ) for coupling of four or more E2 operators because of various intermediate couplings. The agreement among them can serve as a measure of convergence in various summations.

Triaxiality from Coulomb excitation experiments: Example of ^{130}Xe

Morrisson et al, PRC 102 (2020) 054304

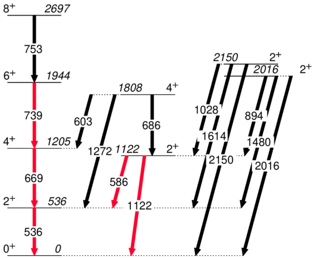

FIG. 4. Low-lying excited states in ^{130}Xe, considered in the present analysis. Transitions observed in the current experiment with a ^{94}Mo target are marked in red. Level and transition energies are given in keV.

Spectroscopic quadrupole moments:

Level	$\langle I\|\|E2\|\|I\rangle$ (eb)	Present
2_1^+	$-0.50(+22,-18)$	$-0.38(+17,-14)$
4_1^+	$-0.55(16)$	$-0.41(12)$
2_2^+	0.1(1)	0.1(1)

State	Component $E2\times E2$	Experiment
0_1^+	$\langle 0_1^+\|\|E2\|\|2_1^+\rangle\langle 2_1^+\|\|E2\|\|0_1^+\rangle$	6240
	$\langle 0_1^+\|\|E2\|\|2_2^+\rangle\langle 2_2^+\|\|E2\|\|0_1^+\rangle$	45
	$\langle 0_1^+\|\|E2\|\|2_3^+\rangle\langle 2_3^+\|\|E2\|\|0_1^+\rangle$	20
	$\langle 0_1^+\|\|E2\|\|2_4^+\rangle\langle 2_4^+\|\|E2\|\|0_1^+\rangle$	45
	$\langle Q^2\rangle$	6350(400)
	$\langle\beta\rangle$	0.17(2)
2_1^+	$\langle 2_1^+\|\|E2\|\|0_1^+\rangle\langle 0_1^+\|\|E2\|\|2_1^+\rangle$	1250
	$\langle 2_1^+\|\|E2\|\|2_2^+\rangle\langle 2_2^+\|\|E2\|\|2_1^+\rangle$	1440
	$\langle 2_1^+\|\|E2\|\|2_3^+\rangle\langle 2_3^+\|\|E2\|\|2_1^+\rangle$	35
	$\langle 2_1^+\|\|E2\|\|2_4^+\rangle\langle 2_4^+\|\|E2\|\|2_1^+\rangle$	5
	$\langle 2_1^+\|\|E2\|\|4_1^+\rangle\langle 4_1^+\|\|E2\|\|2_1^+\rangle$	3350
	$\langle 2_1^+\|\|E2\|\|4_2^+\rangle\langle 4_2^+\|\|E2\|\|2_1^+\rangle$	25
	$\langle 2_1^+\|\|E2\|\|4_3^+\rangle\langle 4_3^+\|\|E2\|\|2_1^+\rangle$	
	$\langle 2_1^+\|\|E2\|\|4_4^+\rangle\langle 4_4^+\|\|E2\|\|2_1^+\rangle$	
	$\langle 2_1^+\|\|E2\|\|3_1^+\rangle\langle 3_1^+\|\|E2\|\|2_1^+\rangle$	
	$\langle 2_1^+\|\|E2\|\|2_1^+\rangle\langle 2_1^+\|\|E2\|\|2_1^+\rangle$	430
	$\langle Q^2\rangle$	6600(400)
	$\langle\beta\rangle$	0.17(2)
	Component $E2\times E2\times E2$	
0_1^+	$\langle 0_1^+\|\|E2\|\|2_1^+\rangle\langle 2_1^+\|\|E2\|\|2_1^+\rangle\langle 2_1^+\|\|E2\|\|0_1^+\rangle$	−312 050
	$\langle 0_1^+\|\|E2\|\|2_2^+\rangle\langle 2_2^+\|\|E2\|\|2_2^+\rangle\langle 2_2^+\|\|E2\|\|0_1^+\rangle$	450
	$\langle 0_1^+\|\|E2\|\|2_3^+\rangle\langle 2_3^+\|\|E2\|\|2_3^+\rangle\langle 2_3^+\|\|E2\|\|0_1^+\rangle$	2
	$\langle 0_1^+\|\|E2\|\|2_4^+\rangle\langle 2_4^+\|\|E2\|\|2_4^+\rangle\langle 2_4^+\|\|E2\|\|0_1^+\rangle$	0
	$\langle 0_1^+\|\|E2\|\|2_1^+\rangle\langle 2_1^+\|\|E2\|\|2_2^+\rangle\langle 2_2^+\|\|E2\|\|0_1^+\rangle$	45 100
	$\langle 0_1^+\|\|E2\|\|2_1^+\rangle\langle 2_1^+\|\|E2\|\|2_3^+\rangle\langle 2_3^+\|\|E2\|\|0_1^+\rangle$	−4700
	$\langle 0_1^+\|\|E2\|\|2_1^+\rangle\langle 2_1^+\|\|E2\|\|2_4^+\rangle\langle 2_4^+\|\|E2\|\|0_1^+\rangle$	2700
	$\langle 0_1^+\|\|E2\|\|2_2^+\rangle\langle 2_2^+\|\|E2\|\|2_3^+\rangle\langle 2_3^+\|\|E2\|\|0_1^+\rangle$	
	$\langle 0_1^+\|\|E2\|\|2_2^+\rangle\langle 2_2^+\|\|E2\|\|2_4^+\rangle\langle 2_4^+\|\|E2\|\|0_1^+\rangle$	500
	$\langle\cos(3\delta)\rangle$	0.4(2)
	$\langle\gamma\rangle$	23(5)°

Summary

Subjects not covered here:

- Reflection-asymmetric shapes ⇒ talk by L. Robledo
- Rigorous connection between intrinsic states and laboratory observables ⇒ talk by B. Bally
- Data for higher-order multipole moments (there are only very few)
- Fission
- Deformation effects in low-energy nuclear reaction with strongly-interacting probes
- Fine structure of rotational bands and vibrational states
- Neutron distributions from strongly- and weakly-interacting probes

Intrinsic shapes are non-observable for direct measurements, but they leave their fingerprint on virtually all nuclear observables and phenomena

- Structure of excitation spectrum in a given nucleus
- Evolution of excitation spectra
- "Collectivity": rotational and vibrational structures in the excitation spectra, shape coexistence, . . .
- Evolution of charge radii